

peaks. If the speech were derived from a local microphone, a fixed bias might suffice for this. If a distant microphone were employed, however, the bias would have to be derived automatically, since the polarity of the speech wave would be uncertain. Then, also, the frequencies on the line are assumed to be biased by shifting the carrier frequencies, so as to center the peaks of the instantaneous frequencies in the band. Physical means for obtaining these biases could doubtless be devised, if desired.

#### IV. SUMMARY OF RESULTS

Table II gives the swing ratios for the several kinds of automatic level adjustment described above, derived as described from ratios of speech peaks which will be exceeded by 10 per cent of the voices. The computed swing ratio is included in the table for comparison.

TABLE II  
SWING RATIOS FOR SPEECH

| Transmitter | Type of Regulation              | No Filter |     | 3,000-cps Filter |     |
|-------------|---------------------------------|-----------|-----|------------------|-----|
|             |                                 | PM        | FM  | PM               | FM  |
| F1          | Computed in Section 2           | 1.5       | 0.6 |                  |     |
| F1          | A—Constant input volume         | 1.1       | 1.0 | 1.0              | 0.9 |
| F1          | B—Constant peak level of speech | 1.5       | 0.8 | 1.4              | 0.7 |
| F1          | C—Constant phase peaks          | 1.5       | 1.2 | 1.4              | 1.1 |
| F1          | D—Spread centered               | 1.4       | 0.9 | 1.3              | 0.8 |
| Moving-coil | A—Constant input volume         | 1.1       | 0.5 | 0.8              | 0.5 |
| Moving-coil | B—Constant peak level of speech | 1.7       | 0.4 | 1.0              | 0.4 |
| Moving-coil | C—Constant phase peaks          | 1.7       | 0.6 | 1.0              | 0.6 |
| Moving-coil | D—Spreads centered              | 1.3       | 0.5 | 0.8              | 0.5 |

Note: PM = phase modulation. FM = frequency modulation.

#### CONCLUSIONS

In closing, the following comments may be made on the data which have been presented:

(1) The computed swing ratios tend to be equal to or higher than the experimentally determined values for phase modulation, and lower than the experimental values for frequency modulation. This is probably largely because the computation was based on rms speech voltages, while the experimental method was based on measured peak speech voltages.

(2) Of the four methods of volume regulation assumed in analyzing the experimental data, the method of regulating to constant voltage peaks applied to the phase modulator results in the greatest swing ratios, and therefore appears the most efficient in regard to use of the modulator. This is of practical importance, since the greater the efficiency, the higher the carrier frequency at which the modulator may operate, and the fewer the required number of stages of subsequent frequency multiplication.

(3) The 3,000-cps low-pass filter had little effect on the swing ratios, except in the case of the moving-coil microphone and phase modulation.

(4) The moving-coil microphone without any filter gave swing ratios substantially the same as the F1 carbon microphone for phase modulation, but only about half as great for frequency modulation.

A general conclusion is that the swing ratios are quite dependent on the microphone and its circuits, on the kind of volume regulation employed, and probably on other features of the circuit. For accurate results, the swing ratios should therefore be determined for the particular circuits which are to be used. The figures derived here will, however, serve to indicate roughly the values to be expected.

## The Helical Antenna\*

JOHN D. KRAUST†, SENIOR MEMBER, IRE

**Summary**—The helix is a fundamental form of antenna of which loops and straight wires are limiting cases. When the helix is small compared to the wavelength, radiation is maximum normal to the helix axis. Depending on the helix geometry, the radiation may, in theory, be elliptically, plane, or circularly polarized.

When the helix circumference is about 1 wavelength, radiation may be maximum in the direction of the helix axis and circularly polarized or nearly so. This mode of radiation, called the axial or beam mode, is generated in practice with great ease, and may be dominant over a wide frequency range with desirable pattern, impedance, and polarization characteristics. The radiation pattern is

maintained in the axial mode over wide frequency ranges because of a natural adjustment of the phase velocity of wave propagation on the helix. The terminal impedance is relatively constant over the same frequency range because of the large initial attenuation of waves on the helix. The conditions for circular polarization are analyzed, and the importance of the array factor in determining the radiation pattern of a long helix is discussed.

#### INTRODUCTION

**A** HELIX is a fundamental geometric form. It has applications in many branches of physics and engineering. For example, in mechanical systems the helix or coil spring is a familiar structure; in electrical systems, a helical conductor or inductor is a common type of circuit element; and in many dynamic phenom-

\* Decimal classification: R125.1×R326.61. Original manuscript received by the Institute, June 7, 1948. Presented in part, 1948 IRE National Convention, New York, N. Y., March 23, 1948.

† Department of Electrical Engineering, Ohio State University, Columbus, Ohio.

ena, particles follow helical paths. Recently the helix has been applied as a beam antenna.<sup>1-6</sup>

In considering the helix as an antenna, it is important that it be regarded, not as a unique or special form of antenna, but rather as a basic type of which the more familiar loop and straight-wire antennas are merely special cases.<sup>2</sup> Thus, a helix of fixed diameter collapses to a loop as the spacing between turns approaches zero, and, on the other hand, a helix of fixed spacing straightens into a linear conductor as the diameter approaches zero. It is the purpose of this paper to discuss the helical antenna from this general point of view including the axial or beam mode of radiation as a particular case. The possibility of a normal mode of radiation, as suggested by Wheeler,<sup>7</sup> is also included as a special case.

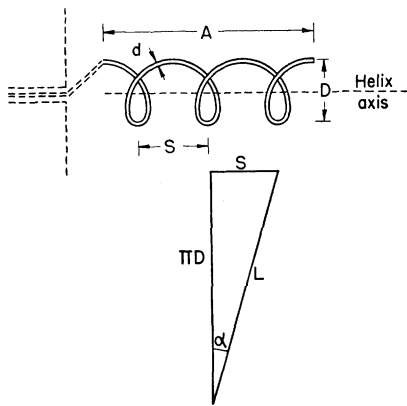


Fig. 1—Relation of helix dimensions.

Referring to Fig. 1, the following symbols will be used to describe a helix:

- $D$  = diameter of helix (center-to-center)
- $S$  = spacing between turns (center-to-center)
- $\alpha$  = pitch angle =  $\arctan S/\pi D$
- $L$  = length of one turn
- $n$  = number of turns
- $A$  = axial length =  $nS$
- $d$  = diameter of helix conductor.

A coaxial transmission line and ground plane as used for exciting the helix in the beam mode of radiation are shown by the dashed lines. A subscript  $\lambda$  signifies that the dimension is measured in free-space wavelengths. For example,  $D_\lambda$  is the helix diameter in free-space wavelengths.

<sup>1</sup> J. D. Kraus, "Helical beam antenna," *Electronics*, vol. 20, pp. 109-111; April, 1947.

<sup>2</sup> J. D. Kraus and J. C. Williamson, "Characteristics of helical antennas radiating in the axial mode," *Jour. Appl. Phys.*, vol. 19, pp. 87-96; January, 1948.

<sup>3</sup> O. J. Glasser and J. D. Kraus, "Measured impedances of helical beam antennas," *Jour. Appl. Phys.*, vol. 19, pp. 193-197; February, 1948.

<sup>4</sup> J. D. Kraus, "Helical beam antennas for wide-band applications," *Proc. I.R.E.*, vol. 36, pp. 1236-1242; October, 1948.

<sup>5</sup> J. D. Kraus, "Design data for helical beam antennas," to be published.

<sup>6</sup> J. D. Kraus, "Measured phase velocities on helical conductors," to be published.

<sup>7</sup> H. A. Wheeler, "A helical antenna for circular polarization," *Proc. I.R.E.*, vol. 35, pp. 1484-1488; December, 1947.

## TRANSMISSION AND RADIATION MODES OF HELICES

The dimensions of a helix are very conveniently illustrated by a diameter versus spacing chart or, as in Fig. 2, by a circumference versus spacing chart. On this chart, the dimensions of a helix may be expressed either in rectangular co-ordinates by the spacing  $S_\lambda$  and circumference  $\pi D_\lambda$  or in polar co-ordinates by the length of one turn  $L_\lambda$  and the pitch angle  $\alpha$ .

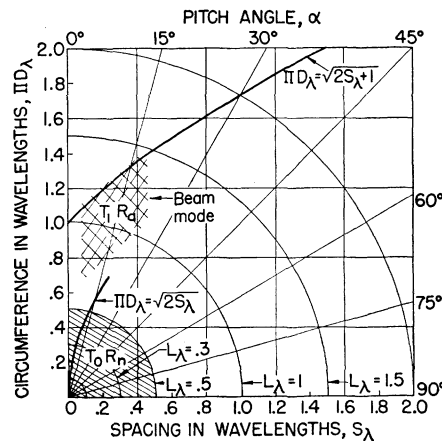


Fig. 2—Circumference versus spacing chart for helices showing regions for normal radiation mode (shaded) and axial or beam mode (cross hatched).

The electromagnetic field around a helix may be regarded from two points of view, as (1) a field which is guided along the helix, and (2) a field which radiates. In the present discussion, it will be convenient to treat these as independent. As regards the first point of view, it is assumed that an electromagnetic wave may be propagated without attenuation along an infinite helix in much the same manner as along an infinite transmission line or waveguide. This propagation may be described by the *transmission mode*, a variety of different modes being possible. On the other hand, a field which radiates may be described by the radiation pattern of the antenna. It will be convenient to classify the general form of the pattern in terms of the direction in which the radiation is a maximum. Although an infinite variety of patterns is possible, two kinds are of particular interest. In one, the direction of the maximum radiation is normal to the helix axis. This is referred to as the *normal radiation mode*<sup>8</sup> or, in shorthand notation, as the  $R_n$  mode. In the other, the direction of maximum radiation is in the direction of the helix axis. This is referred to as the *axial or beam radiation mode*, or, in shorthand notation, as the  $R_a$  mode.

The lowest transmission mode for a helical conductor has adjacent regions of positive and negative charge

<sup>8</sup> The word "mode" is used here in its general sense to indicate merely the general form or type of radiation pattern. In the case of "transmission mode," the word "mode" is employed in a more restricted sense to indicate a particular field configuration. In discussing transmission modes, it is assumed that the helix is infinitely long. However, a radiation pattern implies a helix of finite length, it being assumed that the wave propagates along the finite helix in a particular transmission mode or modes in the same manner as along a portion of an infinite helix, end effects being neglected.

separated by many turns. This mode will be designated as the  $T_0$  mode and the instantaneous charge distribution is suggested by Fig. 3(a). The  $T_0$  mode is important when the length of one turn is small compared to the wavelength  $L \ll \lambda$ , and is the mode commonly occurring

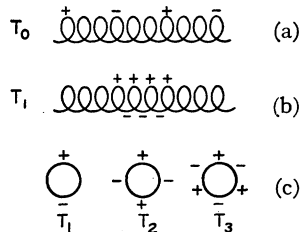


Fig. 3—Approximate charge distribution on helices for different transmission modes.

on low-frequency inductors. It is also the dominant mode in the traveling-wave tube.<sup>9-13</sup> Since the adjacent regions of positive and negative charge are separated by an appreciable axial distance, a substantial axial component of the electric field is present, and in the traveling-wave tube this field interacts with the electron stream. If the criterion  $L_\lambda < \frac{1}{2}$  is arbitrarily selected as a boundary for the  $T_0$  transmission mode, the region of helix dimensions for which this mode is important is shown by the shaded area in Fig. 2.

Theoretically, it is of interest to examine some of the possible radiation patterns associated with the  $T_0$  transmission mode. Only the simplest radiation case will be considered. This occurs when the helix is very short so that  $nL \ll \lambda$  and the assumption is made that the current on the helix is uniform in magnitude and in-phase along its length.<sup>14</sup> Referring to Fig. 3(a), the length is much less than that between adjacent regions of maximum positive and negative charge. Theoretically, it is possible to approximate this condition with a standing wave on a small end-loaded helix. The terminal impedance of such a small helix would be sensitive to frequency and the radiation efficiency would be low. However, let us assume that appreciable radiation can be obtained. The maximum radiation is then normal to the helix axis for all helix dimensions, provided only that  $nL \ll \lambda$ . Hence, this condition is referred to as a normal radiation mode  $R_n$ . Referring to Fig. 4, any component  $E$  of the distant electric field perpendicular to the radius vector is given approximately by  $E = k \sin \theta$ , where  $k$  is a constant. The radiation is, in general, elliptically polarized, but for particular helix dimensions

<sup>9</sup> R. Kompfner, "The traveling-wave tube as amplifier at microwaves," Proc. I.R.E., vol. 35, pp. 124-127; February, 1947.

<sup>10</sup> J. R. Pierce and L. M. Field, "Traveling-wave tubes," Proc. I.R.E., vol. 35, pp. 108-111; February, 1947.

<sup>11</sup> J. R. Pierce, "Theory of the beam-type traveling-wave tube," Proc. I.R.E., vol. 35, pp. 111-123; February, 1947.

<sup>12</sup> L. J. Chu and D. Jackson, "Field theory of traveling-wave tubes," Proc. I.R.E., vol. 36, pp. 853-863; July, 1948.

<sup>13</sup> C. C. Cutler, "Experimental determination of helical-wave properties," Proc. I.R.E., vol. 35, pp. 230-233; February, 1948.

<sup>14</sup> It is assumed here that the phase velocity on the helical conductor is approximately that of light. The in-phase condition requires an infinite phase velocity, but this can be approximated by considering only short helices  $nL \ll \lambda$ .

may be linearly or circularly polarized.<sup>7</sup> These cases are discussed further in a later section (Normal Radiation Mode). We can describe both the transmission mode and radiation pattern for very short, small helices by combining the  $T_0$  transmission mode and the  $R_n$  radiation mode designations as  $T_0R_n$ . This designation is applied to the region of helix dimensions near the origin in Fig. 2.

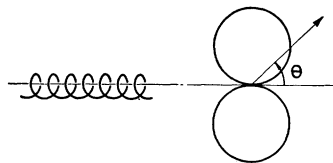


Fig. 4—Sinusoidal field variation for small helices.

A first-order transmission mode, designated  $T_1$ , has adjacent regions of maximum positive and negative electric charge approximately one-half turn apart or near the opposite ends of a diameter, as suggested in Fig. 3(b) for the case of a small pitch angle. This mode is important when the length of one turn is of the order of the wavelength ( $L \sim \lambda$ ). It is found that the radiation from helices of this turn length and of a number of turns ( $n > 1$ ) is usually a maximum in the direction of the helix axis and is circularly polarized, or nearly so.<sup>1,2</sup> This type of radiation pattern is referred to as the axial or beam mode of radiation  $R_a$ . This radiation mode occurs for a wide range of helix dimensions and, being associated with the  $T_1$  transmission mode, the combined designation appropriate to this region of helix dimensions is  $T_1R_a$ . The axial type of radiation is discussed further in a later section (Axial Radiation Mode).

Still higher-order transmission modes, designated  $T_2$ ,  $T_3$ , etc., will have the approximate charge distributions suggested in the one-turn views of Fig. 3(c) for the case of a small pitch angle. For these modes to exist, the length of one turn must generally be at least one wavelength.<sup>15</sup>

The normal  $R_n$  and axial  $R_a$  radiation modes are, in reality, special cases for the radiation patterns of helical antennas. In the general case, the maximum radiation is neither at  $\theta = 0$  nor at  $\theta = 90^\circ$  but at some intermediate value, the pattern being conical or multilobed in form.<sup>2,4</sup>

#### THE NORMAL RADIATION MODE

The direction of maximum radiation is always normal to the helix axis when the helix is small ( $nL \ll \lambda$ ). Referring to Fig. 5(a), the helix is coincident with the polar or  $y$  axis. At a large distance  $r$  from the helix, the electric field may have, in general, two components  $E_\phi$  and  $E_\theta$ , as shown.

Two limiting cases of the small helix are: (1) the short electric dipole of Fig. 5(b),  $\alpha = 90^\circ$ , and (2) the small loop of Fig. 5(c),  $\alpha = 0^\circ$ . In the case of the short electric dipole,  $E_\phi = 0$  everywhere and the distant electric field

<sup>15</sup> The phase velocity along the helical conductor for  $T_1$  and higher modes may differ considerably from that of light. It is often less, and, as shown later, it may be a function of the helix pitch angle and diameter.

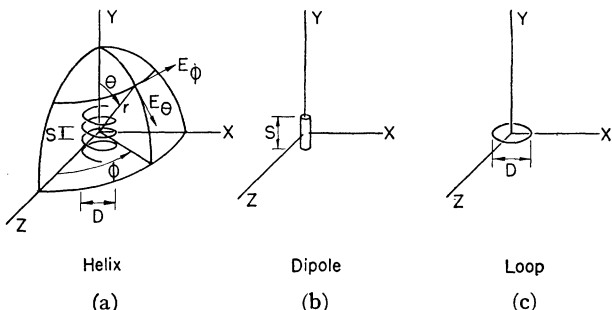


Fig. 5—Relation of field components to helix, dipole, and loop.

has only an  $E_\theta$  component. On the other hand, with the small loop,  $E_\theta=0$  everywhere and the distant electric field has only an  $E_\phi$  component. By the retarded potential method, it may be shown that  $E_\theta$  at a large distance from a short electric dipole ( $r \gg \lambda \gg s$ ) is given by<sup>16,17</sup>

$$E_\theta = \frac{j\omega[I]s \sin \theta}{4\pi\epsilon c^2 r^2} = \frac{j60\pi[I] \sin \theta}{r} \frac{s}{\lambda} \quad (1)$$

where

$s$  = length of short dipole

$\omega = 2\pi f$

$r$  = distance from origin

$c$  = velocity of light (in free space)

$\epsilon$  = dielectric constant of medium (free space)

and  $[I]$  = retarded value of the current =  $I_0 \exp [j\omega(t-r/c)]$ .

In an analogous way,  $E_\phi$  at a large distance from a short magnetic dipole or from the equivalent small loop ( $r \gg \lambda \gg D$ ) is

$$E_\phi = -\frac{120\pi^2[I] \sin \theta}{r} \frac{A}{\lambda^2} \quad (2)$$

where

$A$  = area of loop =  $\pi D^2/4$

$[I]$  = retarded value of the current on the loop.

If  $nL \ll \lambda$ , a helix may be considered, as has been done by Wheeler,<sup>7</sup> to be a combination of a series of loops and linear conductors as illustrated in Fig. 6. Each turn is assumed to consist of a short dipole of length  $S$  connected in series with a small loop of diameter  $D$ . Further, the current on the helix of Fig. 6 is assumed to be uniform and in phase over the entire length. The required end loading is not shown. Provided  $nL \ll \lambda$  where

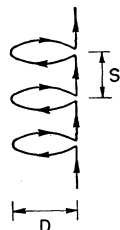


Fig. 6—Equivalent form of small helix.

<sup>16</sup> See, for example, S. Ramo and J. R. Whinnery, "Fields and Waves in Modern Radio," John Wiley and Sons, New York, N. Y., 1944; p. 430.

<sup>17</sup> Rationalized mks units are used.

the length of one "turn" is now given by  $L=S+\pi D$ , the far field pattern will be independent of the number of turns. Hence, to simplify the analysis, only a single turn will be considered. The electric field components at a large distance are then given by (1) and (2). The operator  $j$  in (1) and its absence in (2) indicates that  $E_\phi$  and  $E_\theta$  are in time phase quadrature. Taking the ratio of the magnitudes of  $E_\theta$  and  $E_\phi$ , we have

$$\frac{E_\theta}{E_\phi} = \frac{S\lambda}{2\pi A}. \quad (3)$$

Introducing the relation between the area and diameter of the loop,  $A=\pi D^2/4$ , (3) becomes

$$\frac{E_\theta}{E_\phi} = \frac{2S\lambda}{\pi^2 D^2}. \quad (4)$$

In the general case, both  $E_\theta$  and  $E_\phi$  have values and the electric field is elliptically polarized. Since  $E_\theta$  and  $E_\phi$  are in time phase quadrature, either the major or the minor axis of the polarization ellipse will lie in a plane through the polar or  $y$  axis (see Fig. 5(a)). Let us assume that the  $y$  axis is vertical and that observations of the field are confined to the equatorial or  $x-z$  plane. The ratio of the major to minor axes of the polarization ellipse is conveniently designated as the *axial ratio* (A.R.). Let us define the axial ratio in this case as

$$\text{A.R.} = \frac{E_\theta}{E_\phi} = \frac{2S\lambda}{\pi^2 D^2}. \quad (5)$$

Thus, in the extreme case when  $E_\phi=0$ , the axial ratio is infinite and the polarization ellipse becomes a straight vertical line indicating linear vertical polarization. At the other extreme, when  $E_\theta=0$ , the axial ratio is zero and the polarization ellipse becomes a straight horizontal line indicating linear horizontal polarization.

An interesting special case occurs for an axial ratio of unity ( $E_\theta=E_\phi$ ). This is the case for circular polarization. Setting the axial ratio in (4) equal to 1, we have

$$\pi D = \sqrt{2S\lambda} \quad \text{or} \quad \pi D_\lambda = \sqrt{2S\lambda}. \quad (6)$$

This relation was first shown by Wheeler in an equivalent form.<sup>7</sup> For this case, the polarization ellipse becomes a circle. The radiation is circularly polarized not only in all directions in the  $x-z$  plane but in all directions in space except the direction of the  $\pm y$  axis, where the field is zero.

The relation of helix dimensions for circularly polarized radiation normal to the axis as given by (6) is indicated in Fig. 2, and also in Fig. 7 by the curve marked C.P. (Circular Polarization). This curve is accurate only in the region for which  $\pi D \ll \lambda$  and  $S \ll \lambda$ . This region is shown to an enlarged scale in Fig. 7. In general, the radiation is elliptically polarized. If  $\pi D > \sqrt{2S\lambda}$ , the major axis of the polarization ellipse is horizontal, while if  $\pi D < \sqrt{2S\lambda}$  the major axis is vertical. By varying the pitch angle  $\alpha$  of a helix of constant turn length  $L$ , ori-

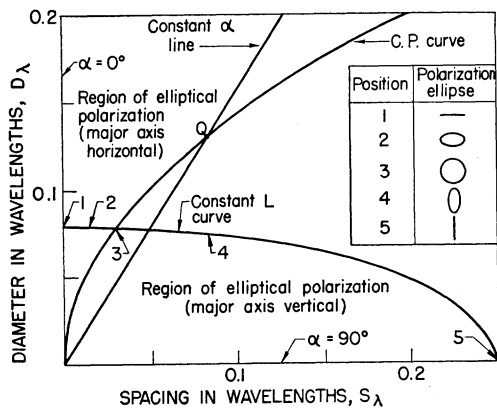


Fig. 7—Diameter versus spacing chart for small helices, showing polarization for different dimensions.

ented as in Fig. 5(a), from the loop case  $\alpha=0^\circ$  as in Fig. 5(c) to the straight conductor case  $\alpha=90^\circ$  as in Fig. 5(b), the radiation changes progressively through the forms listed in Table I.

TABLE I  
NORMAL RADIATION MODE

| Position in Fig. 7 | Condition                               | Radiation  |
|--------------------|---|--|
| (1)                | $S=0$<br>$\alpha=0^\circ$               | Linear (horizontal) polarization   |
| (2)                | $S>0$ and<br>$\pi D > \sqrt{2S\lambda}$ | Elliptical polarization with major axis of polarization ellipse horizontal |
| (3)                | $\pi D = \sqrt{2S\lambda}$              | Circular polarization  |
| (4)                | $0 < \pi D < \sqrt{2S\lambda}$          | Elliptical polarization with major axis of polarization ellipse vertical   |
| (5)                | $\pi D = 0$<br>$\alpha = 90^\circ$      | Linear (vertical) polarization   |

The five conditions of Table I are suggested by the polarization ellipses at the five positions along the constant- $L$  (turn-length) curve in Fig. 7. The fact that the linear polarization is horizontal for the loop and vertical for linear conductors assumes, of course, that the axis of the helix is vertical as in Fig. 5.

For a helix of fixed physical dimensions, the dimensions in wavelengths change along a constant-pitch-angle line as a function of frequency. Thus, as shown in Fig. 7, circularly polarized normal-mode radiation is obtained at only one frequency; that is, where the constant-pitch-angle line for the helix intersects the C.P. curve (point Q in Fig. 7).

In the above discussion of the normal mode of radiation, the assumption is made of a uniform in-phase current along the helical conductor. As already mentioned, this assumption would be approximated if the helix is small ( $nL \ll \lambda$ ). To approximate such a distribution on longer helices would require a phase shifter of some type at intervals along the conductor. This may be inconvenient or impractical.

However, if the assumption of uniform, in-phase current is made without regard as to how it might be pro-

duced, it is interesting to consider some of the above relations further. Although the circularly polarized condition of (6) is true only when  $nL \ll \lambda$ , the relation is nevertheless approximately correct for larger values, say for  $S_\lambda$  and  $D_\lambda$  up to  $\lambda/4$ . The inaccuracy of (6) for large dimensions is due to the deterioration of (1) and (2) when the dipole or the loop are not small. Even if field formulas not restricted to small dipoles or loops are used, another limitation in extending the small-helix equations to helices of larger dimensions is that the simplification of Fig. 6 is no longer adequate. This is because the field of the vertical component of one turn of the helix cannot be properly approximated by a single vertical dipole but must be represented by a series of short dipoles at the circumference of the helix cylinder.

Although there are practical limitations to the application of the normal circularly polarized condition of radiation from a pure helix, an antenna having four slanting dipoles which is suggestive of a modified helix radiating in the normal mode has been built by Brown and Woodward.<sup>18</sup> Their arrangement is based on design principles derived by Lindenblad.<sup>19</sup>

#### AXIAL RADIATION MODE

The preceding section deals mainly with small helices ( $nL \ll \lambda$ ). For this condition, the lowest  $T_0$  transmission mode is dominant and any radiation is in the normal  $R_n$  mode. When the circumference of the helix is increased to about one wavelength ( $\pi D \sim \lambda$ ), the first-order  $T_1$  transmission mode becomes important, and over a considerable range of helix dimensions the radiation may be in the axial  $R_a$  or beam mode.

An outstanding characteristic of the axial or beam mode of radiation is the ease with which it is produced. In fact, owing to the extremely noncritical nature of the helix dimensions in this mode, a helical beam antenna is one of the simplest types of antennas which it is possible to build.

In speaking of transmission modes, it is assumed that the helix is infinite in extent. In discussing radiation modes, the helix must be finite. For convenience, the finite helix is assumed to be in the first approximation a section of an infinite helix. The observed current-dis-

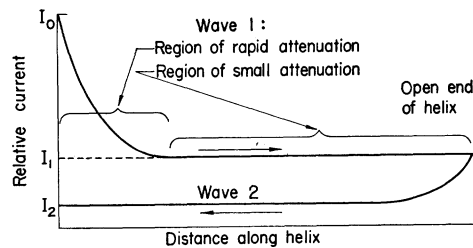


Fig. 8—Resolution of current distribution on the helical beam antenna into current distributions for outgoing and reflected waves. Curves are idealized.

<sup>18</sup> G. H. Brown and O. M. Woodward, "Circularly polarized omnidirectional antenna," *RCA Rev.*, vol. 8, pp. 259-269; June, 1947.

<sup>19</sup> N. E. Lindenblad, "Antennas and transmission lines at the Empire State television station," *Communications*, vol. 21, pp. 13-14; April, 1941.

tribution and terminal-impedance characteristics presented in footnote references 2 and 3 form the basis for making this assumption. Thus the observed current distribution on a helix may be resolved into the current distribution for an outward traveling wave and a current distribution for an inward traveling wave of considerably smaller magnitude, as in Fig. 8. Here each wave is characterized by an initial region of relatively rapid attenuation which is followed by a region in which the current is relatively constant in value. Hallén<sup>20</sup> has pointed out that a similar type of current distribution is characteristic for a traveling wave on a straight cylindrical conductor. Current-distribution measurements on long-straight cylindrical conductors by Bhargava,<sup>21</sup> when resolved into distributions for two traveling waves, indicate that the initial attenuation is greater for conductors of large diameter. In comparing the current distributions on straight cylindrical conductors and on helical conductors, it appears that a relatively thin conductor of diameter  $d$ , wound as a helix, has a current distribution with an initial attenuation for the component traveling waves as large as that on a straight cylindrical conductor of much greater diameter. The helix must, of course, be radiating in the beam mode for this to be the case. This large attenuation of the reflected wave on the helical conductor results in the relatively uniform current distribution over the central region of long helices. The marked attenuation of both the outgoing and reflected waves also accounts for the relatively stable terminal impedance of a helical antenna radiating in the axial mode, since relatively little energy reflected from the open end of the helix reaches the input. Thus the SWR of current at the input terminals is

$$SWR = \frac{I_0 + I_2}{I_0 - I_2}.$$

Since  $I_2$  is small compared to  $I_0$  (see Fig. 8), the SWR at the input terminals is nearly unity, the same as for a transmission line terminated in approximately its characteristic impedance.

When the helix is radiating in the axial mode, the phase velocity of wave propagation on the helix is such as to make the component electric fields from each turn of the helix add nearly in phase in the direction of the helix axis. The tendency for this to occur is sufficiently strong that the phase velocity adjusts itself to produce this result. This natural adjustment of the phase velocity is one of the important characteristics of wave transmission in the  $T_1$  mode on a helix. It is this fact which accounts for the persistence of axial-mode  $R_a$  radiation patterns over such a wide frequency range. The phase velocity of wave propagation along a helical conductor is approximately equal to the velocity of light in free

<sup>20</sup> Erik Hallén, private communication to the author, March 25, 1948.

<sup>21</sup> B. N. Bhargava, "A study of current distribution on long radiators," master's thesis, Department of Electrical Engineering, Ohio State University, Columbus, Ohio; 1947.

space  $c$  when the frequency is too low for the axial  $R_a$  mode of radiation. As the frequency is increased, it is found that there is a frequency range in which the phase velocity is decreased. In this same frequency range, the radiation is observed to be in the axial  $R_a$  mode and the current distribution changes from that due to two nearly equal but oppositely directed traveling waves, to essentially a single outgoing traveling wave and a small reflected wave, as in Fig. 8.

#### ARRAY FACTOR

As an approximation, a helical antenna radiating in the axial mode can be assumed to have a single uniform traveling wave on its conductor. Based on this assumption, an approximate expression for the field pattern of a single-turn helix is developed in footnote reference 2. The pattern of a helix of a number of turns is then calculated as an array of such turns by taking the product of the pattern for the single turn and for the array. When the helix is sufficiently long ( $nS$  large), the array factor is dominant and largely determines the shape of the helix pattern. Calculated and measured patterns for a helix of 7 turns and  $12^\circ$  pitch angle ( $n=7, \alpha=12^\circ$ ) are compared in Fig. 21 of footnote reference 2. As an example which illustrates the dominant effect of the array factor, the component electric field patterns for this case are presented in Fig. 9. In this figure,

$E_{\phi T}$  = pattern of horizontally polarized component for one turn

$E_{\theta T}$  = pattern of vertically polarized component for one turn

$Y_n$  = pattern of array of seven ( $n=7$ ) isotropic point sources spaced 0.225 wavelength ( $S_\lambda=0.225$ ) and for phase-velocity factor  $\beta=0.83$ .

$E_\phi = E_{\phi T} Y_n$  = pattern of horizontally polarized component of electric field from entire helix

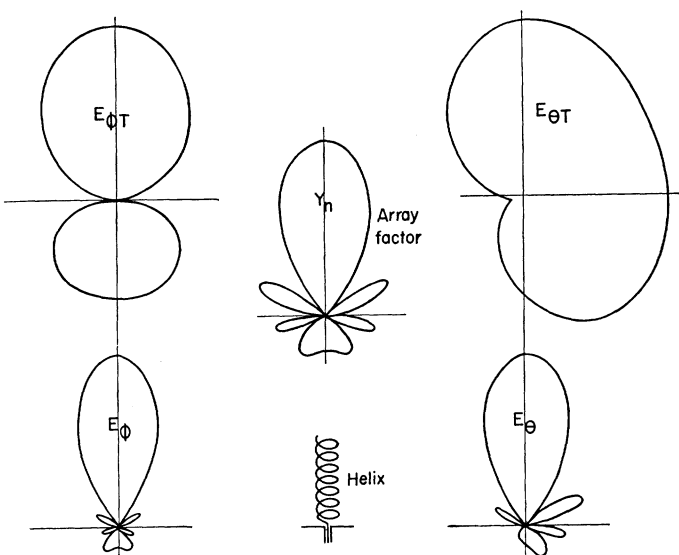


Fig. 9—Patterns  $E_\phi$  and  $E_\theta$  for a seven-turn  $12^\circ$  helix as calculated from the array factor  $Y_n$  for an array of seven isotropic point sources and the single-turn patterns  $E_{\phi T}$  and  $E_{\theta T}$ .

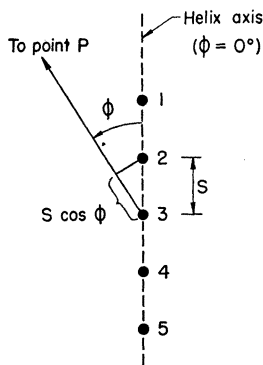


Fig. 10—Linear array of isotropic point sources.

$E_\theta = E_{\theta T} Y_n$  = pattern of vertically polarized component of electric field from entire helix.

It is interesting to note that, although the patterns of the horizontally and vertically polarized components for a single turn are very different in form, the patterns of the horizontally and vertically polarized components for the entire helix are nearly the same.<sup>22</sup> Furthermore, the main lobes of the  $E_\theta$  and  $E_\phi$  patterns are very similar to the array-factor pattern. Thus it is apparent that, for long helices, a calculation of the array factor alone suffices for the approximate helix pattern in any polarization.

To calculate the array factor, a helix of  $n$  turns is replaced by  $n$  isotropic point sources separated by the spacing  $S$  between turns of the helix. An array of  $n$  point sources is illustrated by Fig. 10. The normalized array factor (maximum value unity) is then given by equations (18) and (19) of footnote reference 2, or more simply by<sup>23</sup>

$$Y_n = \frac{1}{n} \frac{\sin \frac{n\psi}{2}}{\sin \frac{\psi}{2}} \quad (7)$$

where  $n$  = any integer ( $1, 2, 3, \dots$ ), and  $\psi$  is an auxiliary function giving the phase difference between successive sources in a particular direction  $\phi$ . For  $\psi = 0$ , (7) is indeterminate, so that in this case it is necessary to take  $Y_n$  in the limit as  $\psi$  approaches zero. The phase of the wave arriving at a distant point  $P$  due to source 1 is advanced over the phase of the wave from source 2 by  $2\pi S_\lambda \cos \phi$ , but is retarded by  $2\pi L_\lambda / p$ . This retardation is proportional to the length of time required for a wave to travel around one turn or from source 2 to 1.

The value of  $\psi$  is then the difference of these. Thus,

$$\psi = 2\pi \left( S_\lambda \cos \phi - \frac{L_\lambda}{p} \right) \quad (8)$$

<sup>22</sup> The calculated  $E_\theta$  pattern of Fig. 21, footnote reference 2, is a mirror image along the helix axis of the  $E_\theta$  pattern in Fig. 9. The image was taken in footnote reference 2 to allow a direct comparison between the left-handed helix used in the calculations and the right-handed helix which was measured.

<sup>23</sup> S. A. Schelkunoff, "Electromagnetic Waves," D. Van Nostrand Co., Inc., New York, N. Y., 1943; p. 342.

where

$S_\lambda$  = spacing between helix turns in free-space wavelengths

$\phi$  = direction angle with respect to helix axis

$L_\lambda$  = length of one helix turn in free-space wavelengths

$p$  = phase velocity factor =  $v/c$ , or

$$p = \frac{\text{phase velocity along helix conductor}}{\text{velocity of light in free space}}. \quad (9)$$

It is interesting to examine the case for which the fields from the sources arrive at a remote point on the axis in the same phase; that is, when  $\psi = -2\pi m$  and  $\phi = 0$ , where  $m$  is any integer ( $0, 1, 2, \dots$ ). Then,

$$\frac{L_\lambda}{p} = m + S_\lambda. \quad (9)$$

When  $m = 1$ , we have the approximate relation for the  $T_1$  transmission mode:<sup>24</sup>

$$\frac{L_\lambda}{p} = 1 + S_\lambda \quad \text{or} \quad \frac{L}{p} = \lambda + S, \quad (10)$$

and, if  $p = 1$ ,  $L - S = \lambda$ . Equation (10) is a fair approximation for helical antennas radiating in the axial mode. The phase difference is actually observed to be slightly greater, as given by the somewhat better approximation<sup>25</sup>

$$\frac{L_\lambda}{p} = 1 + \frac{1}{2n} + S_\lambda \quad (11)$$

where  $n$  = number of turns. The additional phase shift represented by  $1/2n$  results in sharper helix patterns, as it does also for all end-fire arrays.<sup>26</sup> The additional phase shift is a natural phenomenon in the helical beam antenna and is maintained over a considerable frequency range. The condition of (11) will be referred to as the condition for "maximum directivity."

When  $m = 2$  we have the approximate relation for the  $T_2$  transmission mode:

$$\frac{L_\lambda}{p} = 2 + S_\lambda. \quad (12)$$

The approximate relation for the general  $T_m$  transmission mode of higher order ( $m \geq 1$ ) is as given by (9). If  $p = 1$ , and introducing also the relation  $L^2 = S^2 + \pi^2 D^2$  for a helix, we obtain  $D_\lambda = \sqrt{2mS_\lambda + m^2/\pi}$  and, when  $m = 1$ ,  $D_\lambda = \sqrt{2S_\lambda + 1/\pi}$ .

The diameter versus spacing chart of Fig. 11 has curves of the helix relations for the  $T_1$  transmission

<sup>24</sup> The ratio  $L_\lambda/p$  in (9) and (10) is the length of one turn measured in terms of the wavelength on the helical conductor. This ratio times  $2\pi$  is the phase length of one turn in radians and will be designated  $L_p$ . Thus, from (10) we have  $L_p = 2\pi(1+S_\lambda)$ , which indicates that, for the  $T_1$  transmission mode, one turn has a phase length of  $2\pi$  radians plus  $2\pi S_\lambda$ .

<sup>25</sup> To convert (9) and (11) to radian measure, multiply both sides by  $2\pi$ , while to convert to degrees multiply both sides by  $360$ .

<sup>26</sup> W. W. Hansen and J. R. Woodyard, "A new principle in directional antenna design," Proc. I.R.E., vol. 26, pp. 333-345; March 1938.

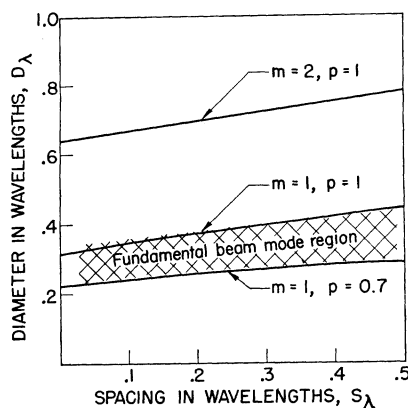


Fig. 11—Diameter versus spacing chart showing region for fundamental axial or beam mode of radiation.

mode for two cases of the phase-velocity factor  $p=1$  and  $p=0.7$ . The cross-hatched area indicates the observed region of the fundamental axial or beam mode of radiation  $R_a$ . The two curves define quite well the upper and lower limits of the region. A curve for a higher-order transmission mode  $T_2$  is also shown in Fig. 11 for the case of  $p=1$ .

Returning to a further consideration of the axial radiation mode, we have from (10), substituting also  $L_\lambda = \pi D_\lambda / \cos \alpha$  and  $S_\lambda = \pi D_\lambda \tan \alpha$ ,

$$p = \frac{L_\lambda}{1 + S_\lambda} = \frac{1}{\left( \tan \alpha + \frac{1}{\pi D_\lambda} \right) \cos \alpha}$$

or

$$p = \frac{1}{\sin \alpha + \frac{\cos \alpha}{\pi D_\lambda}}. \quad (13)$$

Equation (13) gives the required variation in  $p$  for the fields of each turn of a helix of pitch angle  $\alpha$  to add in phase in the axial direction.

In a similar way, we can obtain from (11) the required variation of  $p$  for "maximum directivity" as

$$p = \frac{L_\lambda}{1 + \frac{1}{2n} + S_\lambda} = \frac{1}{\sin \alpha + \left( \frac{2n+1}{2n\pi D_\lambda} \right) \cos \alpha}. \quad (14)$$

#### CONDITIONS FOR CIRCULAR POLARIZATION<sup>27</sup>

In this section, the conditions necessary for circularly polarized radiation in the direction of the helix axis will be analyzed. The discussion is concerned entirely with helices radiating in the axial mode.

Referring to Fig. 12(a), let us consider a helix of diameter  $D = 2r$  having its axis coincident with the  $z$  axis. Expressions will be derived for the electric field at a point  $P$  a large distance  $z_1$  in the direction of the axis of a helical antenna, as shown. The antenna is assumed

<sup>27</sup> In connection with the analysis in this section, it is a pleasure to acknowledge the interest and criticisms of Victor H. Rumsey.

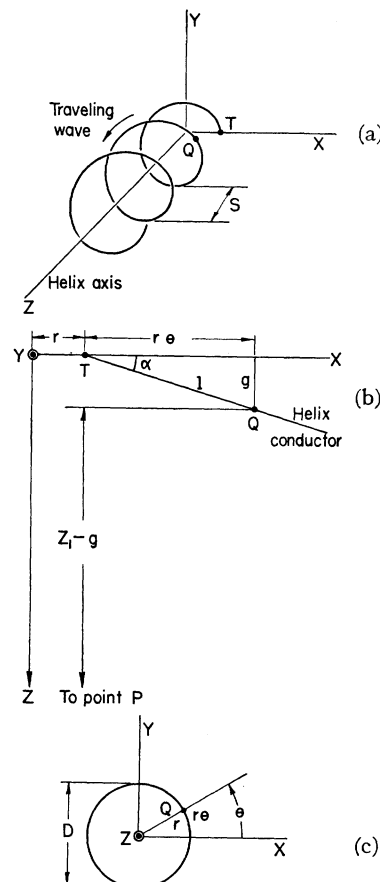


Fig. 12—Relations for analysis of circular-polarization conditions.

to have a single uniform traveling wave. If the helix is unrolled in the  $x$ - $z$  plane, the relations are as indicated in Fig. 12(b). Let point  $Q$  on the helix be a distance  $l$  along the helix from the terminal (point  $T$ ). It is also convenient to specify a cylindrical co-ordinate system as in Fig. 12(c), the angular position of  $Q$  with respect to the  $x$ - $z$  plane being given by  $\theta$ . From the geometry in Fig. 12, we have

$$\left. \begin{aligned} g &= l \sin \alpha \\ z_1 - g &= z_1 - l \sin \alpha \\ \alpha &= \text{arc tan}(S/\pi D) = \text{arc cos}(r\theta/l) \\ r\theta &= l \cos \alpha. \end{aligned} \right\} \quad (15)$$

At a large distance  $z_1$ , the component of the relative electric field intensity in the  $x$  direction  $E_x$  for a helix of an integral number of turns  $n$  is given by

$$E_x = E_0 \int_0^{2\pi n} \sin \theta e^{i\omega(t-z_1/c + (l \sin \alpha)/c - l/p_c)} d\theta \quad (16)$$

where

- $E_0$  = a constant involving the current magnitude on the helix
- $c$  = velocity of light in free space ( $3 \times 10^8$  meters/second)
- $t$  = time in seconds
- $\omega = 2\pi$  (frequency)

$p$ =phase-velocity factor= $v/c$ , where

$v$ =phase velocity of wave propagating along helical conductor.

Using the relations of (15), the last two terms of the exponent may be re-expressed:

$$\frac{l \sin \alpha}{c} - \frac{l}{pc} = \frac{r\theta}{c} \left( \tan \alpha - \frac{1}{p \cos \alpha} \right) = \frac{r\theta b}{c} \quad (17)$$

where

$$b = \tan \alpha - \frac{1}{p \cos \alpha}.$$

For  $\alpha=0$ , we have a loop, and  $b=-1/p$ . Hence, the relation being derived may be applied not only to the general helix case but also the special case of a loop. Since  $t$  and  $z_1$  are independent of  $\theta$ , the first two terms of the exponent may be taken outside the integral. Hence (16) becomes

$$E_x = E_0 e^{j(\omega t - \beta z_1)} \int_0^{2\pi n} \sin \theta e^{jk\theta} d\theta \quad (18)$$

where

$$\beta = 2\pi/\lambda$$

$$k = \beta r b = L_\lambda \left( \sin \alpha - \frac{1}{p} \right). \quad (19)$$

Integrating and introducing limits, we obtain

$$E_x = \frac{E_1}{k^2 - 1} (e^{j2\pi n k} - 1) \quad (20)$$

where

$$E_1 = E_0 e^{j(\omega t - \beta z_1)}.$$

The expression for the relative electric field intensity in the  $y$  direction  $E_y$  is identical to (20) except that it has  $\cos \theta$  instead of  $\sin \theta$ . From this we obtain

$$E_y = \frac{E_1 k}{j(k^2 - 1)} (e^{j2\pi n k} - 1). \quad (21)$$

For circular polarization on the axis, the required condition is

$$\frac{E_x}{E_y} = \pm j. \quad (22)$$

Taking the ratio of  $E_x$  to  $E_y$  as given by (20) and (21), we get

$$\frac{E_x}{E_y} = \frac{j}{k}. \quad (23)$$

Hence, for circular polarization on the axis of a helix of an integral number of turns ( $n=1, 2, 3, \dots$ ),  $k$  must equal  $\pm 1$ .

However, as will be shown, nearly circular polarization may be obtained provided only that the helix is

long and  $k$  is nearly unity. For this case, the number of turns may assume nonintegral values. Hence, the length of the helical conductor will be specified as  $\theta_1$  instead of  $2\pi n$ . Thus, rewriting (18), we have

$$E_x = \frac{E_1}{2j} \int_0^{\theta_1} [e^{j(k+1)\theta} - e^{j(k-1)\theta}] d\theta \quad (24)$$

which becomes, after integrating, introducing the condition  $k \sim -1$ , and the approximation for  $k+1 \sim 0$  that  $e^{j(k+1)\theta_1} \approx 1 + j(k+1)\theta_1$ ,

$$E_x = - \frac{E_1}{2} \left[ j\theta_1 - \frac{e^{j(k-1)\theta_1} - 1}{k - 1} \right]. \quad (25)$$

In a similar fashion, we obtain for the relative electric field intensity component in the  $y$  direction,  $E_y$ :

$$E_y = \frac{E_1}{2j} \left[ j\theta_1 + \frac{e^{j(k-1)\theta_1} - 1}{k - 1} \right]. \quad (26)$$

If the helix is very long ( $\theta_1 \gg 1$ ), (25) and (26) become very nearly

$$E_x = -j \frac{E_1 \theta_1}{2} \quad \text{and} \quad E_y = \frac{E_1 \theta_1}{2}. \quad (27)$$

The ratio of these then gives  $E_x/E_y = -j$ , which satisfies the condition for circular polarization. Although these give the important conditions for circular polarization, another condition resulting in circular polarization is obtained when  $(k \pm 1)\theta_1 = 2\pi m$  where  $m$ =integer. This condition is fulfilled when either the positive or negative sign in  $(k \pm 1)$  is chosen, but not for both. To summarize the important conditions:<sup>28</sup>

(1) The radiation in the axial direction from a helical antenna of any pitch angle ( $0 < \alpha < 90^\circ$ ) and of an integral number of one or more turns will be circularly polarized if  $k = \pm 1$ .

(2) The radiation in the axial direction from a helical antenna of any pitch angle ( $0 < \alpha < 90^\circ$ ) and a large number of turns, which are not necessarily an integral number, is nearly circularly polarized if  $k$  is nearly  $\pm 1$ .

Let us now investigate the significance of the requirement that  $k = \pm 1$ . Referring to (19),  $k$  is negative in the case of interest, since  $\sin \alpha \leq 1$  and  $1/p \geq 1$ . Thus, for  $k = -1$  we have

$$L_\lambda \left( \sin \alpha - \frac{1}{p} \right) = -1$$

or

$$p = \frac{L_\lambda}{L_\lambda \sin \alpha + 1} = \frac{L_\lambda}{S_\lambda + 1}. \quad (28)$$

If  $p=1$ , the circular polarization condition is  $L_\lambda - S_\lambda = 1$  or  $L - S = \lambda$ . This was first pointed out in footnote reference 1. The relation for  $p$  in (28) is identical with the

<sup>28</sup> A single, traveling wave (1 in Fig. 8) is assumed on the helix and the effect of the reflected wave (2 in Fig. 8) is neglected. The effect of the reflected wave on the axial ratio is discussed in footnote reference 2, p. 91.

value of  $p$  required for the fields of each turn of a helix to add in phase in the axial direction as given by (13).<sup>29</sup>

#### PHASE-VELOCITY COMPARISON

Several expressions for the required phase-velocity factor  $p$  have been derived corresponding to different conditions. These are summarized for the  $T_1$  transmission mode in Table II. Two of the expressions are identical, namely, for circular polarization (C.P.), and in-phase fields from each turn. In Table II,  $\phi_0$  is the value of  $\phi$  at the first null in the radiation pattern, and  $\psi_0$  is the value of  $\psi$  at the first null in the array factor.

TABLE II

| Condition   | Required Phase-Velocity Factor $p$  |
|---|---|
| (1) and (2) C.P. and in-phase fields                  | $p = \frac{L_\lambda}{S_\lambda + 1} = \frac{1}{\sin \alpha + \frac{\cos \alpha}{\pi D_\lambda}}$   |
| (3) Maximum directivity                               | $p = \frac{L_\lambda}{S_\lambda + 1 + \frac{1}{2n}} = \frac{1}{\sin \alpha + \left(\frac{2n+1}{2n}\right) \frac{\cos \alpha}{\pi D_\lambda}}$ |
| (4) From first null of measured pattern <sup>30</sup> | $p = \frac{L_\lambda}{S_\lambda \cos \phi_0 + 1 + \frac{\psi_0}{2\pi}}$   |

Curves calculated by the three different methods of Table II are compared in Fig. 13 with the measured variation of the phase velocity as a function of frequency on a seven-turn  $12^\circ$  helix.<sup>31</sup> All curves are in general agreement in the region in which  $p$  increases with frequency.<sup>32</sup> In Fig. 13, 300 Mc corresponds to a helix circumference of 0.72 free-space wavelengths and 500 Mc to a helix circumference of 1.2 free-space wavelengths. It can be effectively demonstrated that  $p$  for "maximum directivity" is most probably the one actually occurring on the

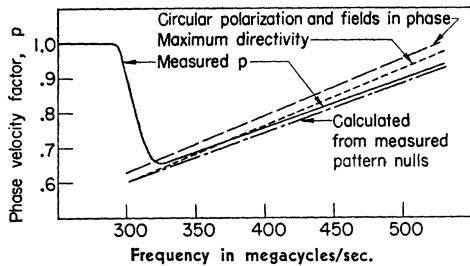


Fig. 13—Comparison of variation of measured phase-velocity factor ( $p = v/c$ ) with frequency on a seven-turn  $12^\circ$  helix with the calculated variation for several conditions.

<sup>29</sup> The condition was expressed in equation (1) of footnote reference 1 as  $L - S = n\lambda$  where  $n$  corresponds to  $m$  in the present paper. Two corrections to footnote reference 1 are that  $n$  may be any integer, not merely an odd integer, and the same condition is not for maximum directivity but for the fields from each turn to add in phase.

<sup>30</sup> See p. 96 of footnote reference 2.

<sup>31</sup> This is the same helix as shown in Fig. 5 of footnote reference 2,  $D=23$  cm.

<sup>32</sup> The agreement of the measured velocity factor with  $p$  for maximum directivity is better than with  $p$  for in-phase fields.

helix by noting the close agreement of measured field patterns with array-factor patterns calculated with this value of  $p$  and the poor agreement when other values of  $p$  are used.

#### SINGLE-TURN PATTERN

The pattern of a single turn is an important factor in determining the pattern of short helices. In the case of long helices, the array factor is relatively more important, and is usually sufficient to give the approximate main-lobe pattern of the helix. However, it is nevertheless necessary that the direction of maximum radiation from a single turn be approximately in the axial direction. Accordingly, it is of interest to investigate briefly the form of the single-turn pattern of helical antennas radiating in the axial mode. Referring to the preceding sections, the condition  $k = -1$  also results in the single-turn pattern maximum being nearly in the axial direction. This follows from the fact that when  $\alpha$  is small the length of a turn is nearly one wavelength, so that the instantaneous current directions on a single turn are as shown in Fig. 14(a). If  $\alpha$  is small, this is approximately equivalent at one instant of time to a broadside array of two short dipoles spaced by about the diameter of the helix, as in Fig. 14(b). Since the dipoles are in phase, the maximum radiation is normal to their plane or in the axial direction. The pattern is also very broad in the axial direction, as indicated. With passage of time, these equivalent dipoles rotate around the axis, yielding circular polarization. If  $\alpha$  is not small, then it becomes necessary to approximate the single turn of the helix by a square turn with four short linear segments, as was done in the pattern calculations of footnote reference 2. A square turn is suggested by the perspective sketch in Fig. 14(c). Since the wave on the helix is, to a good approximation a single, traveling wave, the radiation maximum is tilted forward from the normal to the conductor. As shown in footnote reference 2, it turns out that the tilt angle  $\tau$  of the radiation maximum for a short segment ( $D \sim 0.3\lambda$ ) is of the order of  $10^\circ$ . When  $\alpha = \tau$ , the radiation maximum for each segment is in the axial direction (Fig. 14(d)). Adding the fields of the segments gives the single-turn pattern.

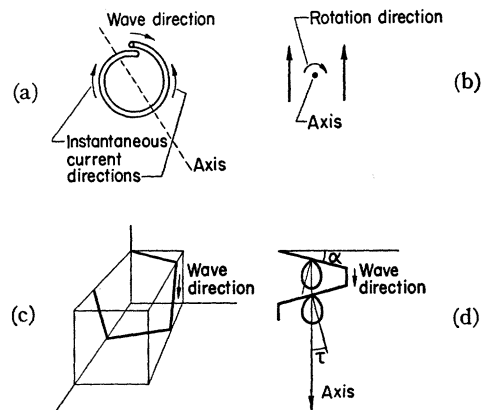


Fig. 14—Relations for discussion on pattern of single turn.